

Ultrafast carrier dynamics of Si quantum dots embedded in SiN matrix

Lap Van Dao,^{a)} Jeff Davis, and Peter Hannaford
*Centre for Atom Optics and Ultrafast Spectroscopy, Swinburne University of Technology,
 and ARC Centre of Excellence for Coherent X-Ray Science, Swinburne University of Technology,
 Melbourne, 3122 Australia*

Young-Hyun Cho, Martin A. Green, and Eun-Chel Cho
*Centre of Excellence for Advanced Silicon Photovoltaics and Photonics, The University of New South
 Wales, Sydney, 2052 Australia*

(Received 8 November 2006; accepted 19 January 2007; published online 21 February 2007)

Femtosecond spectrally resolved two-color three-pulse nonlinear spectroscopy is used to study the dynamics and coherence properties of excited carriers in Si quantum dot structures embedded in silicon nitride. A very short dephasing time of <180 fs at room temperature is observed. Ultrashort population relaxation times of ~ 400 fs and 6–10 ps are measured and discussed in the context of the different contributions from transverse optical and transverse acoustic phonon-assisted transitions. © 2007 American Institute of Physics. [DOI: 10.1063/1.2695977]

The investigation of semiconductor quantum structures, such as quantum dots, has attracted much attention in recent years for fundamental research and device applications.¹ The development of devices based on quantum structures requires an understanding of the optical properties, such as decoherence, radiative lifetimes, mechanisms of coherent coupling, and interaction with the phonon bath. Spectroscopic methods, especially time resolved spectroscopy techniques, such as pump-probe,² time resolved photoluminescence,^{3–5} four-wave mixing, and photon echoes,^{6–9} have proven to be powerful tools for studying the optical properties of quantum structures.

The development of efficient silicon light-emitting materials based on silicon nanostructures opens a new phase for applications related to the optoelectronic properties of silicon, which has been the backbone of advances in electronics for several decades. Quantum dot (QD) structures in a SiO₂ matrix have been fabricated previously and their optical properties have been studied.^{5,10} In dielectric matrices, the effective mobility of carriers in the QDs and the tunneling between them depends on the spacing of the QDs. Transport properties are also expected to depend on the matrix in which the silicon quantum dots are embedded. The tunneling probability is strongly dependent on the height of the barriers. Si₃N₄ and SiC give lower barriers than SiO₂, allowing a larger dot spacing for a given current.¹¹

When quantum dots are built from direct-gap semiconductors, e.g., InAs, the low-temperature photoluminescence is characterized by sharp spikes confirming the atomic-like nature of the emitting states. However, for indirect-gap semiconductor quantum dots, such as silicon, the emission and absorption spectra are more complex.^{12,13} In indirect-gap *bulk* materials, the purely electronic optical transition at the band edge is forbidden due to momentum conservation requirements, and only phonon-assisted transitions can occur. In quantum structures, the \mathbf{k} selection rule is broken^{14,15} and both zero-phonon and phonon-assisted transitions can contribute to the optical properties near the band edge. The multiphonon broadening by low acoustic-phonon modes is sub-

stantial, and hence the total broadening is large and the emission and absorption spectra from small silicon QDs do not correspond to sharp spikes.¹⁶ The relative contributions and influence of zero-phonon and phonon-assisted transitions on the optical properties of Si QDs are not well understood and require more detailed study.

In this letter we use femtosecond spectrally resolved two-color three-pulse nonlinear spectroscopy to study the dynamics and coherence properties of excited carriers in Si QD structures embedded in silicon nitride (SiN). A very short dephasing time, the ultrashort decay times of “hot” excited carriers, and the contribution of different phonon modes in the carrier dynamics are deduced and discussed.

In the three-pulse nonlinear spectroscopy used here, three ultrashort pulses with pulse widths of about 100 fs are used, two pump pulses with wave vectors \mathbf{k}_1 and \mathbf{k}_2 , wavelength $\lambda_1 = \lambda_2$ and time delay between them t_{12} , and a probe pulse with wave vector \mathbf{k}_3 , time delay t_{23} (between pulses \mathbf{k}_2 and \mathbf{k}_3) and wavelength λ_3 which can be different from or the same as λ_1 . The nonlinear signal generated in the phase matched directions, e.g., $\mathbf{k}_4 = -\mathbf{k}_1 + \mathbf{k}_2 + \mathbf{k}_3$, can, to some approximation, be considered to arise from the third-order polarization and is analyzed on this basis.^{17–19} In our experiment the signal is detected in the reflected direction of \mathbf{k}_4 by a spectrometer equipped with a charge coupled device array (spectral resolution <1 nm) and measured over a range of fixed delay times t_{12} or t_{23} while scanning the other delay time t_{23} or t_{12} , respectively. Positive time is defined as when the \mathbf{k}_2 pulse precedes \mathbf{k}_1 for the t_{12} delay or \mathbf{k}_3 for the t_{23} delay.

The sample for this study consists of ten bilayers of Si quantum dot superlattices in a nitride matrix. A typical high resolution transmission electron microscope image shows spherical Si nanocrystalline quantum dots with 4 nm diameter.

The peak at about 600 nm (see inset in Fig. 2) in the photoluminescence and inverse reflection spectra (which are similar to absorption spectra) is assigned to the band-edge transition. With the pump wavelength (laser pulses \mathbf{k}_1 and \mathbf{k}_2) at 600 nm, we expect that the laser pulse generates carriers predominantly around the band edge. With the pump wavelength at 545 nm, we expect that the laser pulse inter-

^{a)}Electronic mail: dvlap@swin.edu.au

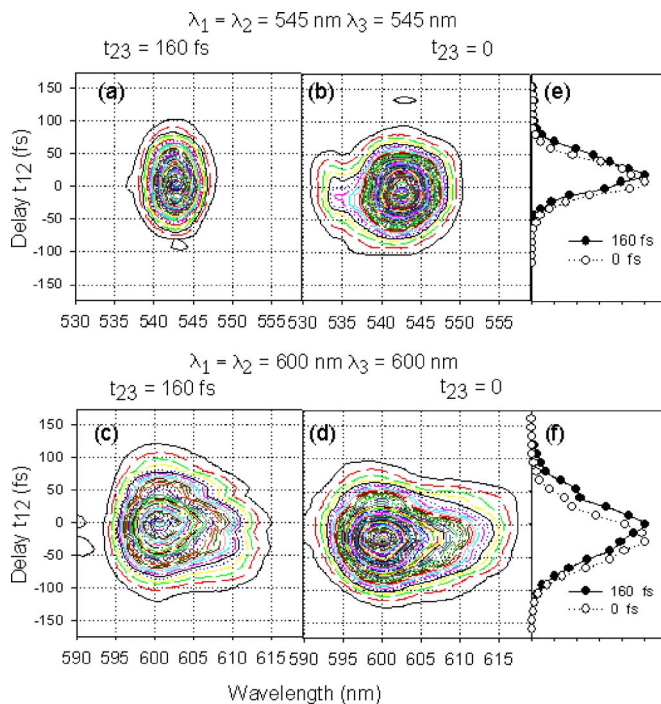


FIG. 1. (Color online) Spectra of three-pulse nonlinear signals vs delay time t_{12} . The delay t_{23} is fixed at 160 fs [(a) and (c)] or 0 fs [(b) and (d)]. The wavelengths of the laser pulses are 545 nm [(a) and (b)] and 600 nm [(c) and (d)]. The time evolution of the signal intensity at 545 nm (e) and 600 nm (f) is recorded with a spectral window of 2 nm.

acts with phonon-assisted transitions to the band edge and with transitions whose energy is higher than that of the conduction band minimum, hence generating either electrons and holes with large excess energy (hot electrons/holes) or an increased phonon density.

Let us discuss scanning of delay time t_{12} , the dephasing time. When the wavelengths of the pump and probe (k_3) pulses are the same, the coherent interaction of the laser pulse and the excited system is strongest, and this is the case in the experiments discussed below, where the cases of 545 and 600 nm excitations are discussed.

For a fixed delay $t_{23}=160$ fs a symmetric intensity profile centered at $t_{12}=0$ with a decay time of ~ 40 fs (for both positive and negative time delays) as a function of t_{12} is detected, as seen in Figs. 1(e) and 1(f). The signal spectrum [Figs. 1(a) and 1(c)], which is the same as the spectrum of the probe pulse, indicates that the observed signal involves the diffraction of the probe pulse by the grating induced by the two pump pulses, and that the spectrally integrated signal [Figs. 1(e) and 1(f)] reflects the time profile of the laser pulse. For a fixed delay $t_{23}=0$ a slight extension of the signal to negative delay t_{12} and a peak shift¹⁹ are seen, as shown in Figs. 1(e) and 1(f). For $t_{23}=0$, the negative delay of t_{12} favors rephasing processes and a photon echo signal can be generated.¹⁹ The amplitude of the photon echo signal is expected to decay as a function of t_{12} , with a decay rate of $4/T_2$,¹⁸ where T_2 is the dephasing time. While the difference of the time profiles for the fixed delays at $t_{23}=0$ and $t_{23}=160$ fs [Figs. 1(e) and 1(f)] is small, the peak shift on the time axis and the difference in the spectra for the two cases is clear [Figs. 1(a)–1(d)]. The broadening of the spectrum and the peak shift for $t_{23}=0$ indicate that the detected signal in this case is not simply the diffraction of the probe pulse and that an additional signal is generated in the sample from

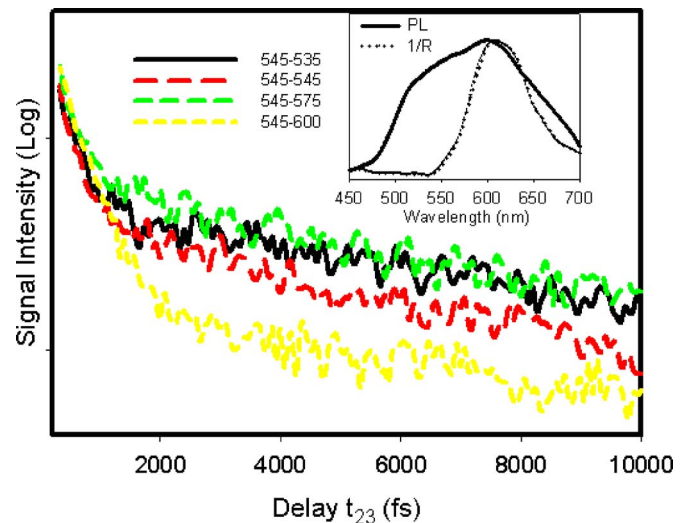


FIG. 2. (Color online) Time evolution of the signal intensity vs delay time t_{23} with $t_{12}=0$ for different probe wavelengths. The pump wavelength is 545 nm. The inset shows the photoluminescence (PL) and inverse reflection (1/R) spectra at room temperature.

induced nonlinear polarization,¹⁸ and hence there is some finite dephasing time for the probed transitions. Based on the assumption that the signal at negative t_{12} , with a decay time of ~ 45 fs, contains a photon echo on top of the contribution from the overlap of the laser pulses, a dephasing time $T_2 < 180$ fs is obtained.

Let us discuss scanning of the population time t_{23} . The time evolution of the nonlinear signal versus delay t_{23} provides information about the relaxation time of excited carriers. By studying the relaxation dynamics in this way, the excited states are probed directly, as opposed to time resolved photoluminescence which relies on the radiative emission of the excited carriers. This is particularly interesting in Si QD systems where there is a combination of phonon-assisted and zero-phonon transitions.^{15,20–22}

In crystalline Si, different phonon modes, i.e., the transverse optical (TO), longitudinal optical (LO), and transverse acoustic (TA) phonon modes, with a maximum phonon energy of 65 meV,¹⁶ can contribute to the optical properties. The TO modes dominate the phonon-assisted optical transitions in weakly confined nanocrystalline Si with small contributions from LO and TA phonons.^{15,20,21} Experimental studies²¹ and theoretical calculations¹⁶ show that the ratio of optical to acoustic phonon-assisted processes is of the order of 10 and appears to be independent of the confinement energy.¹⁶

In this study, the two pump pulses are set to 545 nm and the wavelengths of the probe pulse are 535, 545, 575, and 600 nm. The nonlinear (transient grating) signals detected in these experiments, with $t_{12}=0$, are shown in Fig. 2 as a function of delay t_{23} . In all cases, a rapid rise time that does not vary with different probe wavelengths is observed. This suggests that the same electronic states are being probed in each case and that the carriers are generated in a hot phonon bath.

Following the rapid rise, there are three decay components present, two of which are clearly apparent in Fig. 2 and a much longer lived (>50 ps) component that appears as an offset in these results. It has been shown previously⁵ that the lifetime of excited carriers in such systems is of the order of microseconds, and so it is expected that this contributes to

the slow component. In this type of experiment there is an additional mechanism by which the signal can decay, that of diffusion and drift of the carriers. Experiments in which the angle between the two pump beams (and hence the transient grating period) is varied indicate that the two short lived components observed in Fig. 2 are independent of the grating period; however, the decay rate of the longer lived component (>50 ps) does actually vary as a result of the diffusion of carriers, as discussed in detail elsewhere.²³ Fits to the experimental data using two exponentials with a long decay (>50 ps) as an offset show that the shorter decay occurs with a lifetime of approximately 400 fs and is essentially independent of excitation wavelength. The lifetime for the other decay component does, however, vary with increasing probe wavelength, giving values of 6.5, 6.5, 7.5, and 10 ps for probe wavelengths of 535, 545, 575, and 600 nm, respectively.

From previous studies of intraband transitions in direct-gap semiconductors, it is expected that the optical phonons emit and decay on a short time scale.²⁴ Based on this assumption, the short lifetime (~ 400 fs) is attributed to the rapid decay of the TO phonon density. This decay of TO phonons leads to a decrease in the efficiency of the corresponding phonon-assisted transition being probed, which manifests as a change in the complex refractive index of the sample and so is observed in the detected nonlinear signal. The ratio of the amplitude of the short (400 fs) to the long (>6.5 ps) decays is in the range of 8–11 for probe wavelengths of 535, 545, and 575 nm. This ratio is roughly equivalent to the value of 10 predicted for the ratio of the transition probabilities of TO to TA phonon-assisted transitions. This observation suggests that the longer lived component may be due to the decay of the TA phonons generated by the excitation, observed through the TA phonon-assisted transition. This is supported by the observed decrease in the decay rate of this slower component with increasing probe wavelength, which is explained as follows: Following excitation at 545 nm the phonon density is high, and this is expected to decay over time, leading to a decay in the signal due to phonon-assisted transitions and relaxation of optical phonons into acoustic phonons.²⁵ As the wavelength of the probe is increased, the acoustic-phonon density increases and fewer phonons are required to assist the transition, i.e., multiphonon processes decrease, and the decay of the signal is slower.

When the sample is probed with 600 nm pulses, several other processes become important, e.g., zero-phonon transitions, and it is no longer possible to separate the different regions of the decay into specific transitions.

In conclusion, two-color three-pulse spectrally resolved nonlinear spectroscopy has been used to study the carrier

dynamics in Si quantum dots embedded in SiN. The strong phonon scattering leads to very short dephasing times of <180 fs. Decay of the TO phonon population and the localization of hot carriers contribute to a short decay observed through the TO phonon-assisted transitions, and the decay of TA phonons leads to a longer decay component. From these results the different contributions of TO and TA phonon-assisted transitions to the carrier dynamics can be separated.

The authors gratefully acknowledge the Australian Research Council for financial support.

- ¹P. Chen, C. Piermarocchi, and L. J. Sham, *Phys. Rev. Lett.* **87**, 067401 (2001).
- ²T. H. Tievater, X. Li, D. G. Steel, D. Gammon, D. S. Kazer, D. Park, C. Piermarocchi, and L. J. Sham, *Phys. Rev. Lett.* **87**, 133603 (2001).
- ³H. Kamada, H. Gotoh, J. Temmyo, T. Takagahara, and H. Ando, *Phys. Rev. Lett.* **87**, 246401 (2001).
- ⁴A. V. Baranov, V. Davydov, A. V. Fedorov, H. W. Ren, S. Sugou, and Y. Masumoto, *Phys. Status Solidi B* **224**, 461 (2001).
- ⁵L. V. Dao, X. Wen, M. T. T. Do, P. Hannaford, E. Cho, Y. Cho, and Y. Huang, *J. Appl. Phys.* **97**, 013501 (2005).
- ⁶L. V. Dao, M. Lowe, P. Hannaford, H. Makino, T. Takai, and T. Yao, *Appl. Phys. Lett.* **81**, 1806 (2002).
- ⁷A. Vagov, V. M. Axt, and T. Kuhn, *Phys. Rev. B* **67**, 115338 (2003).
- ⁸N. H. Bonadeo, J. Erland, D. Gammon, D. Park, D. S. Katzer, and D. G. Steel, *Science* **282**, 1473 (1998).
- ⁹A. E. Colonna, X. Yang, and G. D. Scholes, *Phys. Status Solidi B* **242**, 990 (2005).
- ¹⁰Y. H. Cho, M. A. Green, E. C. Cho, Y. Huang, T. Trupke, and G. Conibeer, *Proceedings of the 20th European Photovoltaic Solar Energy Conference*, Barcelona, Spain, June 2005 (in press), p. 47.
- ¹¹C.-W. Jiang and M. A. Green, *J. Appl. Phys.* **99**, 114902 (2006).
- ¹²G. Ledoux, O. Guillois, D. Porterat, C. Reynaud, F. Huisken, B. Kohn, and V. Paillard, *Phys. Rev. B* **62**, 15942 (2000).
- ¹³I. Sychugov, R. Juhasz, J. Valenta, and J. Linnros, *Phys. Rev. Lett.* **94**, 087405 (2005).
- ¹⁴C. Delerue, G. Allan, and M. Lannoo, *Phys. Rev.* **48**, 11024 (1993).
- ¹⁵D. Kovalev, H. Heckler, M. Ben-Chorin, G. Polisski, M. Schwartzkopff, and F. Koch, *Phys. Rev. Lett.* **81**, 2803 (1998).
- ¹⁶C. Delerue, G. Allan, and M. Lannoo, *Phys. Rev. B* **64**, 193402 (2001).
- ¹⁷L. V. Dao, C. N. Lincoln, R. M. Lowe, and P. Hannaford, *J. Chem. Phys.* **120**, 8434 (2004); *Femtosecond Laser Spectroscopy* (Springer, New York, 2005), Chap. 8, p. 197.
- ¹⁸W. Zinth and W. Kaiser, *Topics in Applied Physics* (Springer, Heidelberg, 1988), Vol. 60, Chap. 6, p. 235.
- ¹⁹S. Mukamel, *Principles of Nonlinear Optical Spectroscopy* (Oxford University Press, New York, 1995), Chap. 10, 289.
- ²⁰M. S. Hybertsen, *Phys. Rev. Lett.* **72**, 1514 (1994).
- ²¹D. Kovalev, H. Heckler, B. Averboukh, M. Ben-Chorin, M. Schwartzkopff, and F. Koch, *Phys. Rev. B* **57**, 3741 (1998).
- ²²C. Delerue, G. Allan, C. Reynaud, O. Guillois, G. Ledoux, and F. Huisken, *Phys. Rev. B* **73**, 235318 (2006).
- ²³H. J. Eichler, P. Gunter, and W. Pohn, *Laser Induced Dynamics Grating* (Springer, Heidelberg, 1986), Chap. 4, p. 80.
- ²⁴J. A. Kash, J. C. Tsang, and J. M. Hvam, *Phys. Rev. Lett.* **54**, 2151 (1985).
- ²⁵F. Vallée and F. Bogani, *Phys. Rev. B* **43**, 12049 (1991).